High-field magnetic behavior and forced-ferromagnetic state in an $ErFe_{11}TiH$ single crystal

N. V. Kostyuchenko and A. K. Zvezdin
A. M. Prokhorov General Physics Institute of Russian Academy of Sciences, Moscow 119991, Russia; and Moscow Institute of Physics and Technology, Dolgoprudny, Moscow Region 141700, Russia

E. A. Tereshina*
Institute of Physics CAS, 18221 Prague, Czech Republic

Y. Skourski
Hochfeld-Magnetlabor Dresden (HLD-EMFL), Helmholtz-Zentrum Dresden-Rossendorf, Dresden, Germany

M. Doerr
Technische Universität Dresden, D-01062 Dresden, Germany

H. Drulis
Institute of Low Temperature and Structure Research, 50-950 Wroclaw, Poland

I. A. Pelevin and I. S. Tereshina
Baikov Institute of Metallurgy and Materials Science RAS, 119991 Moscow, Russia; International Laboratory of High Magnetic Fields and Low Temperatures PAS, 53-421 Wroclaw, Poland; and Faculty of Physics, Lomonosov Moscow State University, 119991 Moscow, Russia

(Received 26 June 2015; revised manuscript received 28 July 2015; published 21 September 2015)

The crystal-field and exchange parameters are determined for the single-crystalline hydride $ErFe_{11}TiH$ compound by analyzing the experimental magnetization curves obtained in magnetic fields of up to 60 T. By using the calculated parameters we succeeded in modeling theoretical magnetization curves for $ErFe_{11}TiH$ up to 200 T and to study in detail the transition from ferrimagnetic to a ferromagnetic state in the applied magnetic field.

DOI: 10.1103/PhysRevB.92.104423 PACS number(s): 75.10.Dg, 75.30.Gw, 75.50.Bb, 75.60.Ej

I. INTRODUCTION

The demand on commercially viable high-energy magnets stimulates the studies of perspective materials by different means, including the use of high magnetic fields. A series of 4*f*-3*d* ferromagnets (usually light rare-earths (*R*) Nd and Sm are used as the 4*f* metals while the 3*d* element is Fe or Co) remains the strongest in many applications [1–4]. These materials possess high saturation magnetization M_s and Curie temperature, T_C, and their large uniaxial magnetic anisotropy, provided by the *R* sublattice, is a keystone of a high-coercive state. In order to unleash the magnetic potential of ferrimagnets (heavy *R*'s have large magnetic moments oriented antiparallel to those of the 3*d* sublattice) by inducing the ferromagnetic state, sufficiently high magnetic fields should be used. The conditions, at which a forced-ferromagnetic state is reached, give full information on the strength of the *R*-Fe intersublattice coupling [5–7].

The most rich in iron, quasibinary $RFe_{11}Ti$-type alloys with a rather simple crystal structure of the $ThMn_{12}$ type [8] have a single atomic position for the *R* atom and three nonequivalent Fe lattice sites (Fig. 1) (cf. with two Nd positions and six Fe sites in the famous permanent magnet $Nd_2Fe_{14}B$ [3]). This simplifies theoretical description of the magnetic properties. At the same time, functional magnetic properties, initially inferior to those of $Nd_2Fe_{14}B$ [3], can be improved significantly by doping $RFe_{11}Ti$ interstitially with nitrogen, carbon, or hydrogen [9,10].

Limited experimental capabilities in the past allowed for obtaining the magnetization data for $RFe_{11}Ti$ in rather low magnetic fields only (pulsed fields up to 30 T or 14 T steady fields) while stronger magnetic fields are required for reliable theoretical description of the intersublattice exchange processes in the two-sublattice ferrimagnets. The studies in high magnetic fields up to 60–100 T became feasible on a regular basis only recently [7,11]. Skourski *et al.* [12] investigated the magnetization of $HoFe_{11}Ti$ and $ErFe_{11}Ti$ single crystals in fields up to 60 T and observed a series of field-induced transitions in the magnetization curves. In the present work, we have made use of the fact that light interstitial atoms weaken the *R*-Fe exchange [10] and studied the high-field magnetization processes in the hydrogen-doped $ErFe_{11}Ti$ single crystal. The crystal field (CF) and exchange interaction parameters were determined using the experimental data collected up to 60 T. By employing the calculated parameters we succeeded in modeling theoretical magnetization curves for $ErFe_{11}TiH$ up to 200 T. This allowed us to study in detail the field-induced transition from ferrimagnetic to a ferromagnetic state taking place in the magnetic field exceeding 60 T.

II. EXPERIMENTAL DETAILS AND RESULTS

The polycrystalline ingots of $ErFe_{11}Ti$ were obtained by induction melting of constituent elements with the purity of at least 99.95 wt.% under an argon atmosphere as described

*teresh@fzu.cz

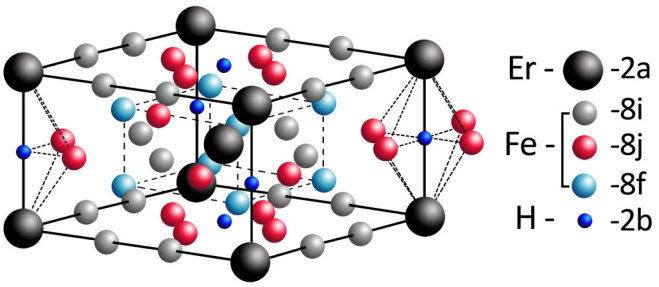

FIG. 1. (Color online) Crystal structure of $ErFe_{11}TiH$.

in Ref. [12]. To stimulate growth of single-crystalline grains, the ingots were remelted and cooled slowly in a resistance furnace with a high temperature gradient. The single crystal blocks weighing a few milligrams were then picked out of the crushed ingots. The single-crystalline state of the samples was confirmed using a conventional back Laue reflection method. The misalignment of crystallographic axes in monocrystalline grains did not exceed 5–7 degrees. The samples were further subjected to hydrogenation in a stainless steel chamber. A special temperature program has been applied in order to preserve the single-crystalline state of $ErFe_{11}Ti$ after hydrogenation. A short thermal activation process at 420 °C in high vacuum was carried out to initiate the hydrogen absorption process and was completed by a one-hour cooling to 20 °C. After that, the reaction chamber was filled in with high-purity hydrogen gas under 1 atm pressure and the system was heated to 350 °C. The samples were annealed in the hydrogen atmosphere for 12 hours and cooled slowly down to room temperature. The amount of absorbed hydrogen was determined from the hydrogen pressure change in the calibrated reactor chamber after finishing the hydrogenation reaction. $ErFe_{11}TiH_{1-y}$ ($y \approx 0.02$) with hydrogen concentration close to one hydrogen atom per formula unit (H at./f.u.) were synthesized. Single crystals of $ErFe_{11}TiH_{1-y}$ hydrides remained of good quality as was confirmed by x-ray back-scattering Laue patterns.

High-field magnetization measurements at 4.2 K were carried out in pulsed magnetic fields up to 60 T using the equipment of the High-Field Laboratory at Dresden-Rossendorf. The pulsed-field data were calibrated using magnetization curves measured on the same samples in static magnetic fields up to 14 T in a commercial PPMS14 magnetometer (Quantum Design, USA). All magnetization curves taken at 4.2 K and presented below were corrected for the demagnetizing field. The Curie temperature has been found using thermomagnetic analysis.

The x-ray powder diffraction analysis showed that $ErFe_{11}Ti$ retained the $ThMn_{12}$-type of crystal structure after hydrogenation. The unit cell volume expanded by 0.8% in $ErFe_{11}TiH$ as compared to the parent $ErFe_{11}Ti$ compound (see Table I) while the Curie temperature increased from 515 to 561 K.

TABLE I. Crystallographic parameters of $ErFe_{11}Ti$ and $ErFe_{11}TiH$.

Compound	a, Å	c, Å	V, Å^3	$\Delta V/V$(%)
$ErFe_{11}Ti$	8.480	4.781	343.8	–
$ErFe_{11}TiH$	8.510	4.785	346.5	0.8

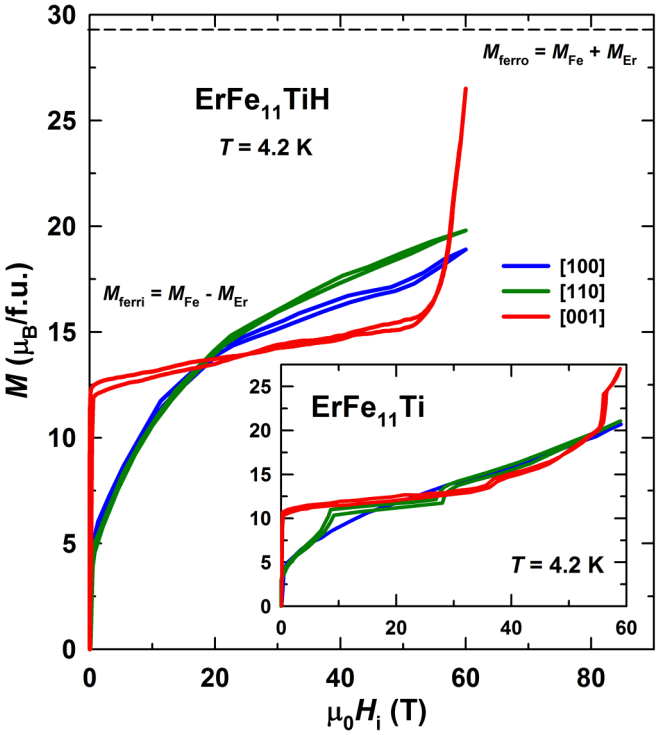

FIG. 2. (Color online) Magnetization curves of an $ErFe_{11}TiH$ single crystal at 4.2 K in fields up to 60 T applied along the main crystallographic directions. Horizontal dashed line is a guide to the eye and shows the saturation magnetization $M_{ferro} = M_{Fe} + M_{Er}$. Inset: the same for the parent $ErFe_{11}Ti$ adopted from Ref. [12].

Figure 2 presents the magnetization curves of an $ErFe_{11}TiH$ single crystal at 4.2 K in magnetic fields up to 60 T applied along the main crystallographic directions. For reference, we show the corresponding data of a parent $ErFe_{11}Ti$ adopted from Ref. [12]. The small amplitude hysteresis observed in the magnetization curves is an artifact and appears due to an integration error at the beginning of the pulse, i.e., at the very high dM/dt [12]. As one can see in Fig. 2, both compounds have nonzero projections of magnetic moment along the [001], [100] and [110] crystallographic axes indicative of the anisotropy of the easy-cone type. It is well known that $RFe_{11}Ti$ and some related rare-earth-iron intermetallics with high iron content may change their anisotropy type after hydrogenation [13–16] but it is not the case of $ErFe_{11}Ti$. Hydrogenation increases the spontaneous magnetization from 10.9 to 11.3 μ_B/f.u., which agrees well with available literature data [17–19].

The largest magnetization jumps in $ErFe_{11}TiH$ and $ErFe_{11}Ti$ for the field applied along the [001] direction are observed at approximately the same magnetic field for the hydride (54 T) and parent (56 T) samples. At the maximum field, the magnetization reaches approximately 26.5 μ_B/f.u. in both compounds. At lower fields, however, the behavior of $ErFe_{11}Ti$ and its hydride is principally different. While the magnetization changes smoothly up to 50 T in $ErFe_{11}TiH$, the magnetization of $ErFe_{11}Ti$ increases significantly at the 35−54 T field range. This influences the magnitude of the magnetization jump. For $ErFe_{11}TiH$ it amounts to 10 μ_B while the magnetization jump is considerably smaller in $ErFe_{11}Ti$.

Smooth magnetization growth along the [100] direction in the basal plane is characteristic for both compounds. The $M(H)$ behavior along the direction [110] is somewhat different for $ErFe_{11}TiH$ and $ErFe_{11}Ti$. The latter features two magnetization steps at ~10 and 27 T whereas the hydrided compound demonstrates the behavior similar to that of the [100] direction.

Since we consider the magnetization at low temperatures, the magnetic moment of an Er sublattice M_{Er} is close to the free-ion value, $9\,\mu_B$/f.u. For the ferrimagnetic (antiparallel) arrangement of Er and Fe moments, the Fe-sublattice moment M_{Fe} is $20.3 \pm 0.1\,\mu_B$/f.u. in $ErFe_{11}TiH$. The magnetic field is a tool to convert the ferrimagnet with $M_{ferri} = M_{Fe} - M_{Er}$ to the field-induced ferromagnet with the saturation moments $M_{ferro} = M_{Fe} + M_{Er}$. In Fig. 2, the magnetization curve of the hydrogenated compound in the [001] direction should saturate at $29.3\,\mu_B$/f.u. (horizontal dashed line). As seen from Fig. 2, the magnetic field slightly exceeding 60 T is required to obtain a ferromagnetic state in $ErFe_{11}TiH$.

III. THEORY

The magnetism of the R-Fe ferrimagnets is provided by the two contributing types of electrons: localized $4f$ electrons of the R sublattice and itinerant $3d$ electrons of the Fe sublattice [2,3]. In order to describe the former, the single-ion approach is used. The compounds with nonmagnetic rare-earth Y and Lu can be employed for evaluation of the iron-sublattice magnetic contribution [20,21]. The exchange interaction between the rare-earth and iron sublattices can be calculated within the mean-field approximation. In comparison with the R-Fe interaction, one may neglect the weakest R-R exchange. The Fe-Fe interaction is the strongest and determines the magnetic ordering temperature of a compound. The magnetic properties of the iron sublattice are characterized by temperature dependences of spontaneous magnetization $M_{Fe}(T)$ and by anisotropy constants of the second and fourth order. The experimentally determined magnetic anisotropy constants at 4.2 K are $K_1 = 2.05\times10^7$ erg/cm^3, $K_2 = 3.57\times10^5$ erg/cm^3 in $YFe_{11}TiH$ [21].

The iron sublattices' contribution to the total free energy is expressed as [22]

$$F_{Fe} = -M_{Fe}(H_x \sin\theta\cos\varphi + H_y \sin\theta\sin\varphi + H_z\cos\theta) + K_1\sin^2\theta + K_2\sin^4\theta. \quad (1)$$

Here, the angles θ and φ are polar coordinates of the iron sublattice magnetization with respect to the main crystallographic directions (c and a axes), $H = (H_x, H_y, H_z)$ is the external magnetic field. The Hamiltonian of the rare-earth ion [3,22,23] is

$$H = H_{CF} + g_J\mu_B \boldsymbol{J}(\boldsymbol{H}_{ex} + \boldsymbol{H}), \quad (2)$$

where g_J is the Landé factor, $\boldsymbol{H}_{ex}$ is the exchange field, $\boldsymbol{J}$ is the total angular momentum of the ground Er^{3+} multiplet. The direction of the exchange field is antiparallel to the iron magnetization. H_{CF} is the crystal field Hamiltonian

$$H_{CF} = B_0^2C_0^2 + B_0^4C_0^4 + B_0^6C_0^6 + B_4^4\left(C_{-4}^4 + C_4^4\right) + B_4^6\left(C_{-4}^6 + C_4^6\right) \quad (3)$$

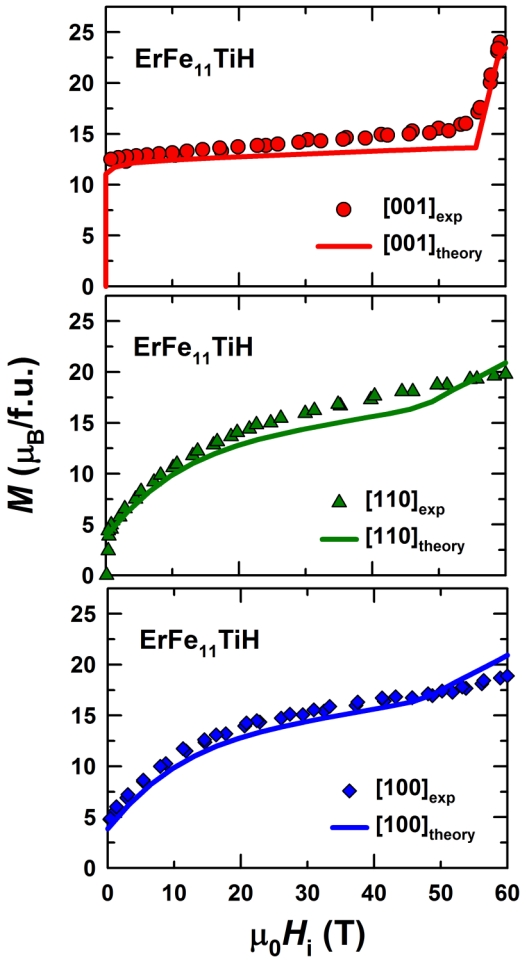

FIG. 3. (Color online) Experimental magnetization isotherms for the $ErFe_{11}TiH$ single crystal obtained along the main crystallographic directions at 4.2 K. Solid lines are the model fit for the set of CF and exchange field parameters determined in this work (see Table I).

with CF parameters B_q^k and single-electron irreducible tensor operators $C_q^k = \sum_i C_q^k(i)$. The rare-earth contribution to the free energy is expressed as

$$F_R = -Nk_BT\log Z, \quad Z = \sum_n \exp\left(\frac{-E_n}{k_BT}\right) \quad (4)$$

for N rare-earth ions. The total free energy of the R-Fe system is then

$$F(\theta,\phi) = -Nk_BT\log Z - M_{Fe}(H_x\sin\theta\cos\varphi + H_y\sin\theta\sin\varphi + H_z\cos\theta) + K_1\sin^2\theta + K_2\sin^4\theta. \quad (5)$$

Numerical values of polar coordinates θ and φ are obtained by minimizing the total free energy at given conditions (temperature, direction and magnitude of external magnetic field). The magnetization behavior of the system obtained by using the following expression:

$$M_\alpha = -\frac{\partial F}{\partial H_\alpha}, \quad \alpha = x,y,z \quad (6)$$

is shown to depend strongly on the crystal-field and exchange parameters. A full set of CF parameters obtained by comparing

TABLE II. CF (in cm^{-1}) and exchange parameters for $ErFe_{11}TiH$ obtained by fitting experimental data in the present work. H_{ex} is shown in T.

B_0^2	B_0^4	B_0^6	B_4^4	B_4^6	H_{ex}
−70	−20	81.85	68.3	0	58.8

theoretical and experimental curves in Fig. 3 is presented in Table II.

IV. DISCUSSION

The crystal-field and exchange parameters define the functional magnetic properties of the rare-earth transition-metal intermetallics, and the elucidation of the parameters is an important task in magnetism. In the present work, 30 000 sets in six-dimensional space were tested in order to find the CF and exchange field parameters, and the magnetization was calculated using Eq. (6) while being compared with the experimental data. As a first step, we used the parameters available in Ref. [14]. However, the obtained theoretical curves (not shown here) were unable to reproduce the high-field experimental magnetization curves. Further, a span of the most probable parameters has been defined, from which the parameters were varied to reach the best fit for all the magnetization curves. By using the experimental high-field magnetization curves we succeeded to obtain a final set of the CF parameters (Table II). Note that B_0^2 is not a dominating parameter in $ErFe_{11}TiH$. The value of the competing parameter B_0^6 (favors the anisotropy of the basal-plane type) is rather large. As the result of hydrogenation, B_0^2 is influenced the most (cf. the parent material in Refs. [14] and [24]) as hydrogen occupies the 2*b* lattice site [25] in the $ThMn_{12}$ crystal structure and has both Er and Fe atoms (8*j* site) as nearest neighbors (Fig. 1). Considerable increase of the *a* lattice parameter as compared to the unchanged parameter *c* in $ErFe_{11}Ti$ after hydrogenation (Table I) decreases the magnetic anisotropy in the basal plane. The effect is mirrored in the coinciding theoretical curves along the [110] and [100] directions up to 60 T (Fig. 3). At the same time, CF parameters B_0^2 and B_0^6 define a proper shape of the curve along the [001] direction. Some discrepancy between the experimental [100] and [110] and the corresponding theoretical curves in Fig. 3 and hence a small anisotropy in the basal plane (Fig. 3) could be due to imperfection in the uniaxiality of the crystal alignment and/or the measurement technique used.

Hydrogenation does not change the cone-of-easy-axes type of magnetic anisotropy at 4.2 K. In both compounds, a spin-reorientation transition toward the *c* axis takes place at elevated temperatures, however, the temperature range where the hydride demonstrates uniaxial anisotropy behavior expands by several tens of degrees [13,18,19]. In other words, hydrogen absorption strengthens uniaxial anisotropy in $ErFe_{11}Ti$.

The study of the field-induced transition from ferrimagnetic to a ferromagnetic state is an equally interesting problem both from fundamental and application viewpoints. In Refs. [26] and [27] it was discussed in detail with respect to rare-earth ferrites. In fact, we are aware of only one occasion of a

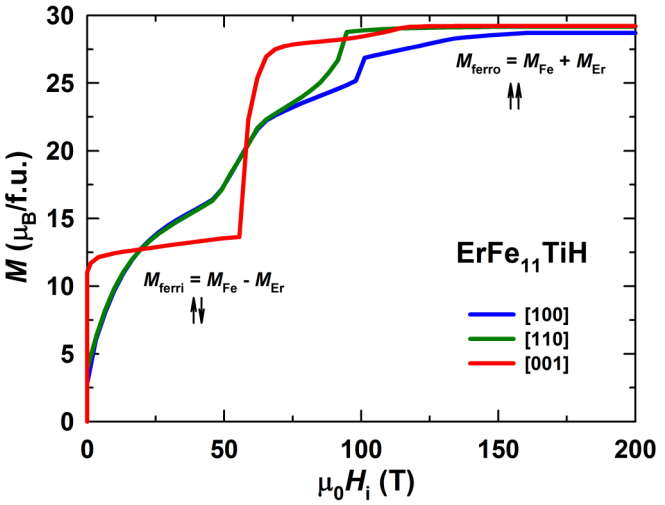

FIG. 4. (Color online) Theoretical magnetization curves plotted using fitted crystal-field parameters from Table II for $ErFe_{11}TiH$ at 4.2 K.

successfully observed forced-ferromagnetic state in rare-earth intermetallic compounds with iron, $Tm_2Fe_{14}B$ [7]. In Ref. [7], the measurements were carried out on a single-crystalline sample along the [100] and [110] directions in fields up to 100 T. The sample reached a forced-ferromagnetic state at about 80 T. The transition was of the second-order type. Another attempt to observe a forced-ferromagnetic state was made in Ref. [28] for Tm_2Fe_{17}. According to the authors' estimation, the system was supposed to reach the ferromagnetic state with the magnetization of 50 μ_B/f.u. but it did not occur even in fields of 74 T. Despite the fact that we also do not observe experimentally the ferromagnetic state in the system at the highest magnetic field applied, we are close to saturating magnetically the $ErFe_{11}TiH$ single crystal (see Fig. 2).

The crystal field and exchange parameters obtained allowed us to construct theoretical magnetization curves for $ErFe_{11}TiH$ up to 200 T. Figure 4 shows the curves along the [100], [110], and [001] crystallographic directions. Our calculations show that the transition toward the forced-ferromagnetic state occurs in the hydride along the [001] direction in the field range of 55–75 T. The full ferromagnetic state requires higher magnetic fields.

V. CONCLUSIONS

The magnetization behavior of a single-crystalline hydride compound $ErFe_{11}TiH$ was studied at 4.2 K using high magnetic fields up to 60 T applied along main crystallographic directions. The data compared to the experimental high-field data of a parent $ErFe_{11}Ti$ sample [12] revealed the effects of hydrogenation on the spin-reorientation transition induced by external magnetic field. The joint experimental magnetic and theoretical efforts allowed us to calculate the crystal field and exchange interaction parameters and to model theoretically the magnetization curves for $ErFe_{11}TiH$ up to 200 T. A complete analysis yields $B_0^2 = -70\,cm^{-1}$, $B_0^4 = -20\,cm^{-1}$, $B_0^6 = 81.85\,cm^{-1}$, $B_4^4 = 68.3\,cm^{-1}$ for $ErFe_{11}TiH$. The competing parameters define the magnetic state of the compound. The exchange field is determined as 58.8 T. In

order to observe a forced-ferromagnetic state in $ErFe_{11}TiH$, fields exceeding 60 T are required.

ACKNOWLEDGMENTS

The authors are grateful to Professor V. S. Rusakov for useful discussions and Dr. K. P. Skokov for $ErFe_{11}Ti$ single crystal preparation. The work is supported by RFBR, Projects No. 13-03-00744, No. 14-03-31395, and No. 15-02-08509. We gratefully acknowledge the support of the HLD at HZDR, member of the European Magnetic Field Laboratory (EMFL). The research of I.A.P and I.S.T was also supported by the project ERA.Net RUS Plus: #146-MAGNES. Part of the measurements has been performed in MLTL (http://mltl.eu) and supported within the program of Czech Research Infrastructures (Project No. LM2011025). N.V.K. and A.K.Z. acknowledge the support of the project 5 top 100 of MIPT(SU).

[1] J. M. D. Coey, *Magnetism and Magnetic Materials* (Cambridge University Press, Cambridge, 2010).
[2] K. H. J. Buschow, in *Handbook of Magnetic Materials*, edited by K. H. J. Buschow (North Holland, Amsterdam, 1997), Vol. 10, p. 463.
[3] J. F. Herbst, Rev. Mod. Phys. **63**, 819 (1991).
[4] E. P. Furlani, *Permanent Magnet and Electromechanical Devices: Materials, Analysis, and Applications* (Academic Press, New York, 2001).
[5] A. V. Andreev, M. D. Kuz'min, Y. Narumi, Y. Skourski, N. V. Kudrevatykh, K. Kindo, F. R. de Boer, and J. Wosnitza, Phys. Rev. B **81**, 134429 (2010).
[6] M. D. Kuz'min and A. K. Zvezdin, J. Appl. Phys. **83**, 3239 (1998).
[7] H. Kato, D. W. Lim, M. Yamada, Y. Nakagawa, H. Aruga Katori, and T. Goto, Physica B **211**, 105 (1995).
[8] W. Suski, in *Handbook on the Physics and Chemistry of Rare Earths*, edited by K. A. Gschneidner and L. Eyring Jr. (Elsevier, Amsterdam, 1996), Vol. 22, p. 143.
[9] H. Fujii and H. Sun, in *Handbook of Magnetic Materials*, edited by K. H. J Buschow (Elsevier, Amsterdam, 1995), Vol. 9, p. 304.
[10] G. Wiesenger and G. Hilcher, in *Handbook of Magnetic Materials*, edited by K. H. J Buschow (Elsevier, Amsterdam, 2008), Vol. 17, p. 293.
[11] S. Zherlitsyn, T. Hermannsdorfer, B. Wustmann, and J. Wosnitza, IEEE Trans. Appl. Supercond. **20**, 672 (2010).
[12] Y. Skourski, J. Bartolomé, M. Kuz'min, K. Skokov, M. Bonilla, O. Gutfleisch, and J. Wosnitza, J. Low Temp. Phys. **170**, 307 (2012).
[13] S. A. Nikitin, I. S. Tereshina, V. N. Verbetsky, and A. A. Salamova, J. Alloys Compd. **316**, 46 (2001).
[14] C. Piquer, F. Grandjean, O. Isnard, and G. J. Long, J. Phys.: Condens. Matter **18**, 221 (2006).
[15] S. A. Nikitin, I. S. Tereshina, N. Y. Pankratov, and Y. V. Skourski, Phys. Rev. B **63**, 134420 (2001).
[16] E. A. Tereshina, H. Drulis, Y. Skourski, and I. S. Tereshina, Phys. Rev. B **87**, 214425 (2013).
[17] O. Isnard and M. Guillot, J. Appl. Phys. **83**, 6730 (1998).
[18] I. Tereshina, S. Nikitin, V. Nikiforov, L. Ponomarenko, V. Verbetsky, A. Salamova, and K. Skokov, J. Alloys Compd. **345**, 16 (2002).
[19] C. Piquer, R. P. Hermann, F. Grandjean, G. J. Long, and O. Isnard, J. Appl. Phys. **93**, 3414 (2003).
[20] L. Y. Zhang and W. E. Wallace, J. Less-Comm. Metals **149**, 371 (1989).
[21] I. S. Tereshina, P. Gaczyński, V. S. Rusakov, H. Drulis, S. A. Nikitin, W. Suski, N. V. Tristan, and T. Palewski, J. Phys.: Condens. Matter **13**, 8161 (2001).
[22] P. Algarabel, M. Ibarra, J. Bartolomé, L. Garcia, and M. Kuz'min, J. Phys.: Condens. Matter **6**, 10551 (1994).
[23] C. Abadia, P. A. Algarabel, B. Garcia-Landa, M. R. Ibarra, A. del Moral, N. V. Kudrevatykh, and P. E. Markin, J. Phys.: Condens. Matter **10**, 349 (1998).
[24] X. C. Kou, T. S. Zhao, R. Grössinger, H. R. Kirchmayr, X. Li, and F. R. De Boer, Phys. Rev. B **47**, 3231 (1993).
[25] O. Isnard and M. Guillot, J. Optoelectron. Adv. Mater. **10**, 744 (2008).
[26] A. K. Zvezdin, in *Handbook of Magnetic Materials*, edited by K. H. J. Buschow (Elsevier, Amsterdam, 1995), Vol. 9, p. 405.
[27] A. K. Zvezdin, in *Encyclopedia of Materials: Science and Technology*, edited by K. H. J. Buschow *et al.* (Elsevier, Amsterdam, 2001), p. 4841.
[28] O. Isnard, A. V. Andreev, M. D. Kuz'min, Y. Skourski, D. I. Gorbunov, J. Wosnitza, N. V. Kudrevatykh, A. Iwasa, A. Kondo, A. Matsuo, and K. Kindo, Phys. Rev. B **88**, 174406 (2013).